From Azobenzene Coordination to Aryl−Halide Bond Activation by Platinum

Olena Zenkina,[†] Marc Altman,[†] Gregory Leitus,[‡] Linda J. W. Shimon,[‡] Revital Cohen,[‡] and Milko E. van der Boom*,[†]

Departments of Organic Chemistry and Chemical Research Support, Weizmann Institute of Science, 76100 Rehovot, Israel

Received May 25, 2007

This contribution describes the reactivity of $Pt(PEt_3)_4$ with (4-bromo-phenyl)-pyridin-4-yl-diazene. η^2-Coordination of $Pt(PEt_3)_2$ to the N═N moiety is kinetically preferable and followed by an aryl−halide bond activation process. This quantitative transformation proceeds under mild reaction conditions in solution and in the solid state. Mechanistic studies in solution indicate that the metal insertion into the aryl−halide bond is the rate-determining step. The reaction obeys first-order kinetics in the η^2-coordination complex with $\Delta G^{\ddagger}_{298K} = 24.6 \pm 1.6$ kcal/mol, $\Delta H^{\ddagger} = 26.5 \pm 1.6$ kcal/mol, and $\Delta S^{\ddagger} = 6.6 \pm 5.0$ eu. No effect on the reaction progress and NMR line shape has been observed in the presence of excess PEt_3. However, competition experiments with the η^2-coordination complex and PhBr reveal that the product ratio can be altered by the presence of PEt_3, indicating that the two aryl−halide bond activation processes proceed via different mechanistic pathways. Numerical analysis of a series of competition experiments fits a reaction scheme involving a unimolecular transformation from the η^2-coordination complex to the product of aryl−halide oxidative addition. This "ring-walking" process is kinetically accessible as shown by density functional theory (DFT) calculations at the PCM:PBE0/SDB-cc-pVDZ/PBE0/SDD level of theory.

Introduction

Aryl−halide bond activation by late transition metals is of prime importance for homogeneous catalysis and metal-mediated synthesis.[1] Metal−arene interactions play a significant role in these processes and may offer new routes for selective bond activation.[2] Seminal work on reaction pathways involving metal−arene interactions was carried out in the 1960s by Basalo.[3] More recent examples include Harman's intramolecular "ring-walking" for various osmium complexes.[4] Stanger and Vollhardt reported on the intramolecular migration of a $(R_3P)_2$-Ni (R = Et, Bu) moiety over an anthracene ligand via a series of $\eta^2-\eta^3$ coordination changes along the system's outer C═C bonds.[5] We reported recently that the reaction of $Pt(PEt_3)_4$ with a halogenated vinylarene results in η^2-C═C coordination, followed by ring-walking of the metal center to give the product of aryl−halide oxidative addition.[6] This pathway to arene functionalization has synthetic utility and might be generalized to selectively activate aryl−halide bonds.[7,8] In a related study, Yokozawa et al. observed that Ni-catalyzed chain growth polymerization of poly(3-hexylthiophene) and poly(*p*-phenylene) proceeds by an intramolecular transfer of the Ni(0) catalyst over the conjugated system, followed by selective activation of a C−Br bond.[9] We provide here in-depth mechanistic insight into metal−ligand coordination followed by an aryl−halide bond activation process by zerovalent platinum. η^2-Coordination of $Pt(PEt_3)_2$ to an N═N moiety is kinetically preferable and followed by rate-determining aryl−halide bond activation (halide = Br, I). This process proceeds quantitatively in solution and in the solid state, and has been studied here by variable-temperature NMR spectroscopy and competition/crossover experiments including numerical analysis. The proposed mechanism is supported by DFT calculations.

* Corresponding author. E-mail: milko.vanderboom@weizmann.ac.il.
[†] Department of Organic Chemistry.
[‡] Department of Chemical Research Support.

(1) (a) Negishi, E. I. *Handbook of Organopalladium Chemistry for Organic Synthesis*; Wiley: New York, 2002. (b) Diederich, F.; Stang, P. J. *Metal catalyzed Cross-Coupling Reactions*; Wiley-VCH, New York, 1998. (c) Hegedus, L. S. *Transition Metals in the Synthesis of Complex Organic Molecules*; University Science Books: Mill Valley, CA, 1994.

(2) (a) Siegel, J. S.; Baldridge, K. K.; Linden, A.; Dorta, R. *J. Am. Chem. Soc.* **2006**, *128*, 10644. (b) Keane, J. M.; Harman, W. D. *Organometallics* **2005**, *24*, 1786. (c) Iverson, C. N.; Lachicotte, R. J.; Müller, C.; Jones, W. D. *Organometallics* **2002**, *21*, 5320. (d) Carbo, J. J.; Eisenstein, O.; Higgitt, C. L.; Klahn, A. H.; Maseras, F.; Oelckers, B.; Perutz, R. N. *Dalton Trans.* **2001**, 1452. (e) Bach, I.; Pörschke, K.-R.; Goddard, R.; Kopiske, C.; Krüger, C.; Rufinska, A.; Seevogel, K. *Organometallics* **1996**, *15*, 4959. (f) Sweet, J. R.; Graham, W. A. G. *Organometallics* **1983**, *2*, 135. (g) Cotton, F. A. *Acc. Chem. Res.* **1968**, *1*, 257.

(3) (a) O'Connor, J. M.; Casey, C. P. *Chem. Rev.* **1987**, *87*, 307. (b) Schuster-Woldan, H. G.; Basolo, F. J. *J. Am. Chem. Soc.* **1966**, *88*, 1657.

(4) Harman, W. D. *Chem. Rev.* **1997**, *97*, 1953.

(5) Stanger, A.; Vollhardt, K. P. C. *Organometallics* **1992**, *11*, 317.

(6) Strawser, D.; Karton, A.; Zenkina, O. V.; Iron, M. A.; Shimon, L. J. W.; Martin, J. M. L.; van der Boom, M. E. *J. Am. Chem. Soc.* **2005**, *127*, 9322. The units reported for the $\Delta S^{\ddagger}$ value is J/K rather than eu. The correct value is $\Delta S^{\ddagger} = -31.1$ eu.

(7) (a) Minami, Y.; Kato, T.; Kuniyasu, H.; Terao, J.; Kambe, N. *Organometallics* **2006**, *25*, 2949. (b) Miyakoshi, R.; Yokoyama, A.; Yokozawa, T. *J. Am. Chem. Soc.* **2005**, *127*, 17542.

(8) For recent examples on aryl−halide bond activation, see: (a) Lucassen, A. C. B.; Shimon, L. J. W.; van der Boom, M. E. *Organometallics* **2006**, *25*, 3308. (b) Grushin, V. V.; Marshall, W. J. *J. Am. Chem. Soc.* **2006**, *128*, 4632. (c) Gatard, S.; Celenligil-Cetin, R.; Guo, C. Y.; Foxman, B. M.; Ozerov, O. V. *J. Am. Chem. Soc.* **2006**, *128*, 2808. (d) Barrios-Landeros, F.; Hartwig, J. F. *J. Am. Chem. Soc.* **2005**, *127*, 6944. (e) Christmann, U.; Vilar, R. *Angew. Chem., Int. Ed.* **2005**, *44*, 366. (f) Fu, G. C. *J. Am. Chem. Soc.* **2002**, *124*, 13662.

(9) (a) Miyakoshi, R.; Shimono, K.; Yokoyama, A.; Yokozawa, T. *J. Am. Chem. Soc.* **2006**, *128*, 16012−16013. (b) Miyakoshi, R.; Yokoyama, A.; Yokozawa, T. *J. Am. Chem. Soc.* **2005**, *127*, 17542−17547.

10.1021/om700519v CCC: $37.00
Publication on Web 07/27/2007

Experimental Section

Materials and Methods. All reactions were carried out in an N_2-filled M. Braun glovebox with H_2O and O_2 levels < 2 ppm. Solvents were reagent grade or better, dried, distilled, and degassed before introduction into the glovebox, where they were stored over activated 4 Å molecular sieves. Deuterated solvents were purchased from Aldrich and were degassed and stored over activated 4 Å molecular sieves in the glovebox. Reaction flasks were washed with deionized water, followed by acetone, and then oven-dried prior to use. Mass spectrometry was carried out using a Micromass Platform LCZ 4000 mass spectrometer. Elemental analyses were performed by H. Kolbe, Mikroanalytisches Laboratorium, Mülheim an der Ruhr, Germany. Ligands **1**, **3**, and **6** were prepared by published procedures.[10]

Spectroscopic Analysis. The ^1H, $^{13}C\{^1H\}$, $^{19}F\{^1H\}$, and $^{31}P\{^1H\}$ NMR spectra were recorded at 400.19, 100.6, 376.5, and 161.9 MHz, respectively, on a Bruker AMX 400 NMR spectrometer. All chemical shifts (δ) are reported in ppm and coupling constants (J) in Hz. The ^1H and ^{13}C NMR chemical shifts are relative to tetramethylsilane; the resonance of the residual protons of the solvent was used as the internal standard h_1 (7.15 ppm, benzene; 5.32 ppm, CH_2Cl_2; 7.09 ppm, toluene; 3.58 and 1.73 ppm, THF) and all-*d* solvent peaks (128.0 ppm, benzene; 54.0 ppm, CH_2Cl_2; 20.4 ppm, toluene; THF, 67.6 and 25.3 ppm). $^{31}P\{^1H\}$ NMR chemical shifts are relative to 85% H_3PO_4 in D_2O at δ 0.0 (external reference), with shifts downfield of the reference considered positive. The ^{19}F NMR spectrum was referenced to external C_6F_6 at $\delta = -162.9$ ppm. All measurements were carried out at 298 K unless stated otherwise. Screw-cap 5 mm NMR tubes were used in NMR follow-up experiments. Assignments in the ^1H and $^{13}C\{^1H\}$ NMR spectra were made using $^1H\{^{31}P\}$ and ^{13}C-DEPT-135 NMR. Temperature calibration of the NMR spectrometer was performed using a mixture of ethyleneglycol with 20% DMSO-d_6. The accuracy of the reported temperatures is ± 0.2 °C.

Formation of Complex 2. A solution of 4-(bromo-phenyl)-pyridin-4-yl-diazene (**1**) (29 mg, 0.11 mmol) in 3 mL of THF was added dropwise to a stirred solution of $Pt(PEt_3)_4$ (75 mg, 0.11 mmol) in 3 mL of THF at room temperature. The quantitative formation of complex **2** was observed by $^{31}P\{^1H\}$ NMR spectroscopy after 30 min. Complex **2** converts selectively to complex **5** in THF at room temperature (~50% conversion after 24 h, ~75% conversion after 96 h) as judged by $^{31}P\{^1H\}$ NMR spectroscopy. ^1H NMR (CD_2Cl_2): δ 8.10 (d, $^3J_{HH} = 5.63$ Hz, 2H, PyrH), 7.18 (t, $^3J_{HH} = 9.7$ Hz, 4H, ArH), 7.14 (d, $^3J_{HH} = 4.72$ Hz, 2H, ArH), 1.68 (m, 12H, PCH_2CH_3), 0.97 (m, 18H, PCH_2CH_3); $^{31}P\{^1H\}$ NMR (THF-d_8): δ 4.92 (d, $^2J_{PP} = 9.11$ Hz, $^1J_{PtP} = 3915.4$ Hz, 1P), 4.7 (d, $^2J_{PP} = 8.95$ Hz, $^1J_{PtP} = 4067.3$ Hz, 1P).

Formation of Complex 4. A solution of $Pt(PEt_3)_4$ (82 mg, 0.12 mmol) in 1 mL of THF was mixed with a THF (2 mL) solution of phenyl-pyridin-4-yl-diazene (**3**) (22 mg, 0.12 mmol) at room temperature. Subsequently, the quantitative formation of complex **4** was observed after 40 min by $^{31}P\{^1H\}$ NMR spectroscopy. Complex **4** was isolated as a dark orange solid by removing all volatiles under vacuum and washing the residue with 10 mL of dry pentane. The remaining solid was dissolved in 0.5 mL of THF followed by addition of pentane (4 mL) and allowed to crystallize by slow evaporation of the solvent under N_2 at room temperature, yielding complex **4** (61 mg, 81%). ^1H NMR (THF-d_8): δ 8.13 (d, $^3J_{HH} = 6.0$ Hz, 2H, PyrH), 7.33 (d, $^3J_{HH} = 7.86$ Hz, 2H, ArH), 7.14 (d, $^3J_{HH} = 3.93$ Hz, 2H, ArH), 7.05 (d, $^3J_{HH} = 7.89$ Hz, 2H, ArH), 6.75 (t, $^3J_{HH} = 7.1$ Hz, 1H, ArH), 1.71 (m, 12H, PCH_2CH_3), 0.98 (m, 18H, PCH_2CH_3). $^{13}C\{^1H\}$ NMR (CD_2Cl_2): δ 165.44 (br, C_q), 158.8 (s, C_q), 151.9 (t, br), 149.8, 128.35, 120.6, 115.1, 18.2 (dd, $^3J_{PC} = 16.7$ Hz, $^1J_{PC} = 47.0$ Hz, $^2J_{PtC} = 30.1$ Hz), 8.5 (d, $^2J_{PC} = 12.6$ Hz, $^3J_{PtC} = 20.25$ Hz). $^{31}P\{^1H\}$ NMR (THF-d_8): δ 5.3 (d, $^2J_{PP} = 5.3$ Hz, $^1J_{PtP} = 3866.5$ Hz, 1P), 5.29 (d, $^2J_{PP} = 5.5$ Hz, $^1J_{PtP} = 4094.0$ Hz, 1P). Calcd *m*/*e*: 614.7, found *m*/*e*: 615.0. Anal. (%) Calcd for $C_{23}H_{39}N_3P_2Pt$: C, 44.95; H, 6.40. Found: C, 44.83; H, 6.35.

Formation of Complex 5. $Pt(PEt_3)_4$ (87 mg, 0.13 mmol) was dissolved in 2 mL of dry THF and slowly added to a stirred solution of (4-bromo-phenyl)-pyridin-4-yl-diazene (**1**) (34 mg, 0.13 mmol) in 3 mL of dry THF. The solution was transferred to a pressure tube, protected from light with aluminum foil, and heated at 40 °C for 14 h. All volatiles were removed under vacuum, and the remaining solid was washed with 15 mL of dry pentane, dried, and redissolved in ~0.5 mL of THF. Subsequently, dry pentane was added dropwise to the THF solution until the complex started to precipitate. Complex **5** was collected as a dark orange-brown solid after 12 h (64 mg, 80%). ^1H NMR (THF-d_8): δ 8.62 (d, $^3J_{HH} = 6.13$ Hz, 2H, PyrH), 7.80 (d, $^3J_{HH} = 8.25$ Hz, 2H, ArH), 7.65 (d, $^3J_{HH} = 8.37$ Hz, 2H, ArH), 7.52 (d, $^3J_{HH} = 6.12$ Hz, 2H, ArH), 1.57 (m, 12H, PCH_2CH_3), 0.88 (m, 18H, PCH_2CH_3). $^{13}C\{^1H\}$ NMR (CD_2Cl_2): δ 158.17 (s, C_q), 154.22 (t, $^3J_{PC} = 18.36$ Hz, C_q), 151.72 (br), 148.89 (br, C_q), 138.85 (t, $^3J_{PC} = 3.5$ Hz, $^2J_{PtC} = 21.50$ Hz), 122.56 (s, $^3J_{PtC} = 21.5$ Hz), 116.28 (s), 14.50 (vt, $^{1+3}J_{PC} = 34.0$ Hz, $^2J_{PtC} = 71$ Hz), 8.01 (s, $^3J_{PtC} = 20.5$ Hz). $^{31}P\{^1H\}$ NMR (THF-d_8): δ 12.02 (s, $^1J_{PtP} = 2721.9$ Hz, 2P). Calc *m*/*e*: 692.1, found *m*/*e* ($M^+ - Br$): 613.5. Anal. (%) calcd for $C_{23}H_{38}BrN_3P_2Pt$: C, 39.83; H, 5.52. Found: C, 39.96; H, 5.45.

Formation of Complex 7. $Pt(PEt_3)_4$ (6.54 mg, 0.0196 mmol) was dissolved in 0.35 mL of dry THF and loaded into a 5 mm screw-cap NMR tube, which was equipped with a septum and sealed with Teflon tape, insulating tape, and Parafilm. A solution of (4-iodo-phenyl)-pyridin-4-yl-diazene (**6**) (3.02 mg, 0.0196 mmol) in 0.35 mL of dry THF was added dropwise into the NMR tube at −75 °C. Subsequently, the NMR tube was shaken and immediately transferred into the cold (−65 °C) NMR spectrometer. The reaction was monitored by $^{31}P\{^1H\}$ NMR spectroscopy, showing the presence of complex **7** at −25 °C. After 1 h, quantitative formation of complex **7** was observed, which is stable at temperatures < 0 °C. For **7**: ^1H NMR (THF-d_8): δ 7.88 (d, $^3J_{HH} = 6.18$ Hz, 2H, PyrH), 7.16 (d, $^3J_{HH} = 8.62$ Hz, 2H, ArH), 6.96 (d, $^3J_{HH} = 7.41$ Hz, 2H, ArH), 6.92 (d, $^3J_{HH} = 5.04$ Hz, 2H, ArH), 1.73 (m, 12H, PCH_2CH_3), 0.87 (m, 18H, PCH_2CH_3). $^{31}P\{^1H\}$ NMR (THF-d_8): δ 3.63 (d, $^2J_{PP} = 4.6$ Hz, $^1J_{PtP} = 3890.5$ Hz, 1P), 3.62 (d, $^2J_{PP} = 4.4$ Hz, $^1J_{PtP} = 4038.6$ Hz, 1P).

Follow-up Experiment of the Formation of Complex 8. The transformation of complex **7** → **8** was monitored by $^{31}P\{^1H\}$ NMR spectroscopy at +15 °C in 1 mL of THF. Formation of complex **8** became visible after approximately 10 min with concurrent disappearance of the starting material (**7**) (10 mg, 0.014 mmol). No other products were observed. After ~17 h, 88% conversion was observed. First-order linear fitting with $R^2 = 0.98$ afforded the rate constant $k_{288K} = -3.5 \times 10^{-5} \pm 7.5 \times 10^{-7}$ s^{-1}. For **8**: ^1H NMR (C_6D_6): δ 8.65 (d, $^3J_{HH} = 6.03$ Hz, 2H, PyrH), 7.87 (d, $^3J_{HH} = 7.22$ Hz, 2H, ArH), 7.65 (d, $^3J_{HH} = 8.37$ Hz, $^3J_{PtH} = 63.6$ Hz, 2H, ArH), 7.55 (d, $^3J_{HH} = 4.54$ Hz, 2H, ArH), 1.63 (m, 12H, PCH_2CH_3), 0.82 (m, 18H, PCH_2CH_3). $^{13}C\{^1H\}$ NMR (C_6D_6): δ 157.6 (s, C_q), 151.6, 148.54 (t, $^3J_{PC} = 3.6$ Hz, C_q), 150.7 (br, C_q), 7.57 (s, $^3J_{PtC} = 25.6$ Hz), 137.59 (t, $^3J_{PC} = 4.88$ Hz, $^2J_{PtC} = 41.93$ Hz), 122.61 (s, $^3J_{PtC} = 78.02$ Hz), 115.89 (s), 15.36 (vt, $^{1+3}J_{PC} = 34.7$ Hz, $^2J_{PtC} = 69.7$ Hz). $^{31}P\{^1H\}$ NMR (THF-d_8): δ 6.7 (s, $^1J_{PtP} = 2678.5$ Hz, 2P). Calcd *m*/*e*: 740.5, found *m*/*e*: 740.7. Anal. (%) Calcd for $C_{23}H_{38}IN_3P_2Pt$: C, 37.31; H, 5.17. Found: C, 37.48; H, 5.14.

Solid-State Formation of Complex 5. The orange powder of compound **2** (30 mg) was heated in a sealed glass pressure tube with exclusion of light at 74 °C under N_2. Importantly, the melting point of the solid is ~120 °C. After 5 days the color of the solid turned dark orange-brown. ^1H and $^{31}P\{^1H\}$ NMR spectroscopy in

(10) Ayyangar, N. R.; Naik, S. N.; Srinivasan, K. V. *Tetrahedron Lett.* **1989**, *30*, 7253.

cold THF-d_8 (−5 °C) showed quantitative conversion of **2** into complex **5** after 11 days. No other products were observed.

$^{31}P\{^1H\}$ NMR Follow-up Experiment of the Formation of 5 from 2. A solution of complex **2** (20 mg, 0.029 mmol) in 1 mL of THF was loaded in a 5 mm screw-cap NMR tube. The reaction progress was monitored by $^{31}P\{^1H\}$ NMR spectroscopy at 40 °C, showing the formation of complex **5** and concurrent disappearance of complex **2**. No intermediates were observed.

$^{31}P\{^1H\}$ NMR Follow-up Competition Experiments of the Formation of Complexes 5 and 12 from Bromobenzene (9) and Complex 2. A solution of bromobenzene (**9**) (4.5 mg, 0.029 mmol) in 1 mL of THF was mixed with a solution of complex **2** (20 mg, 0.029 mmol) in 1 mL of THF and loaded in a 5 mm screw-cap NMR tube. The reaction progress was monitored by $^{31}P\{^1H\}$ NMR spectroscopy, showing the concurrent formation of complexes **5** and **12**[11,12] and the concurrent disappearance of complex **2**. The product ratio **5**:**12** = 5:1 after 14 h (∼99% conversion of starting material). Performing the competition experiment in the presence of 10 equiv of PEt_3 affords a product ratio **5**:**12** = 45:1 after 14 h (∼97% conversion of starting material). Reaction of bromobenzene (0.79 mg/mL, 0.0050 M) in 1 mL of THF with **2** (3.5 mg/mL, 0.0050 M) in 1 mL of THF resulted in the exclusive formation of complex **5** after 14 h (∼97% conversion of starting material. Formation of compound **12** was not observed, suggesting a ratio of **5**:**12** > 65:1. All experiments were conducted at 40 °C.

Competition Experiments of $Pt(PEt_3)_4$ with Bromobenzene (9) and Ligand 1. $Pt(PEt_3)_4$ (15 mg, 0.022 mmol) was dissolved in 3 mL of dry THF and slowly added to a stirred mixture of (4-bromo-phenyl)-pyridin-4-yl-diazene (**1**) (29 mg, 0.11 mmol) and bromobenzene (**9**) (17.6 mg, 0.112 mmol) in 6 mL of dry THF (5-fold excess of each ligand). The solution was transferred to a pressure tube, protected from light with aluminum foil, and heated at 40 °C for 14 h. $^{31}P\{^1H\}$ NMR spectroscopy shows the exclusive formation of product **5**. Formation of compound **12** was not observed. After 14 h, 98% conversion of starting materials was observed, as judged by $^{31}P\{^1H\}$ NMR spectroscopy.

Competition Experiments of $Pt(PEt_3)_4$ with 1-Bromo-4-trifluoromethylbenzene (10) and Ligand 1. $Pt(PEt_3)_4$ (15 mg, 0.022 mmol) was dissolved in 3 mL of dry THF and slowly added to a stirred mixture of (4-bromo-phenyl)-pyridin-4-yl-diazene (**1**) (29 mg, 0.11 mmol) and 1-bromo-4-trifluoromethylbenzene (**10**) (25.3 mg, 0.112 mmol) in 6 mL of dry THF (5-fold excess of each substrate). The solution was transferred to a pressure tube, protected from light with aluminum foil, and heated at 40 °C for 14 h. $^{31}P\{^1H\}$ NMR spectroscopy shows a product ratio **5**:**13** = 2.5:1 (∼99% conversion of starting material). For **13**:[12] ^1H NMR (C_6D_6): δ 7.46 (d, $^3J_{HH}$ = 7.90 Hz, $^3J_{PtH}$ = 65.5 Hz, 2H, ArH), 7.20 (d, $^3J_{HH}$ = 7.93 Hz, 2H, ArH), 1.49 (m, 12H, PCH_2CH_3), 0.84 (m, 18H, PCH_2CH_3). $^{31}P\{^1H\}$ NMR (THF-d_8): δ 12.03 (s, $^1J_{PtP}$ = 2715.5 Hz, 2P). $^{19}F\{^1H\}$ NMR (THF-d_8: δ −62.41, (s, CF_3).

Competition Experiments of $Pt(PEt_3)_4$ with 1-Bromo-4-nitrobenzene (11) and Ligand 1. $Pt(PEt_3)_4$ (15 mg, 0.022 mmol) was dissolved in 3 mL of dry THF and slowly added to a stirred mixture of (4-bromo-phenyl)-pyridin-4-yl-diazene (**1**) (29 mg, 0.11 mmol) and 1-bromo-4-nitrobenzene (**11**) (22 mg, 0.11 mmol) in 6 mL of dry THF (5-fold excess of each substrate). The solution was transferred to a pressure tube, protected from light with aluminum foil, and heated at 40 °C for 14 h. $^{31}P\{^1H\}$ NMR spectroscopy showed a product ratio **5**:**14** = 1:3 after 14 h (∼99% conversion of starting material). For **14**:[12] ^1H NMR (C_6D_6): δ 7.92 (d, $^3J_{HH}$ = 8.44 Hz, 2H, ArH), 6.40 (d, $^3J_{HH}$ = 8.40 Hz, $^3J_{PtH}$ = 63.9 Hz, 2H, ArH), 1.52 (m, 12H, PCH_2CH_3), 0.84 (m, 18H, PCH_2CH_3). $^{13}C\{^1H\}$ NMR (C_6D_6): δ 157.27 (t, C_q), $^2J_{PC}$ = 17.2 Hz), 144.09 (s, C_q), 137.55 (s, $^2J_{PtC}$ = 44.56 Hz), 132,16 (s), 124.77 (s), 120.2 (s, $^2J_{PtC}$ = 79.02 Hz), 14.4 (vt, $^{1+3}J_{PC}$ = 34.2 Hz, J_{PtC} = 69.2 Hz), 7.72 (s, J_{PtC} = 19.56 Hz). $^{31}P\{^1H\}$ NMR (THF-d_8): δ 11.72 (s, $^1J_{PtP}$ = 2675.4 Hz, 2P).

X-ray Analysis of Complex 4. Crystal data: $C_{23}H_{39}N_3P_2Pt$, orange, 0.7 × 0.3 × 0.3 mm^3, orthorhombic, $P2_12_12$, a = 18.851(4) Å, b = 7.919(2) Å, c = 8.342(2) Å, T = 120(2) K, V = 1245.3(4) Å^3, Z = 2, fw = 614.6, D_c = 1.639 Mg·m^{-3}, μ = 5.777 mm^{-1}.

Data collection and processing: Nonius KappaCCD diffractometer, Mo Kα (λ = 0.71073 Å), graphite monochromator, $0 \le h \le 24$, $0 \le k \le 10$, $0 \le l \le 10$, frame scan width = 1°, scan speed 1.0° per 20 s, typical peak mosaicity 0.70°, 12 892 reflections collected, 1614 independent reflections (R_{int} = 0.060). The data were processed with Denzo-Scalepack.

Solution and refinement: The structure has been solved by the Patterson method with SHELXS-97.[13] Full matrix least-squares refinement is based on F^2 with SHELXL-97, 135 parameters with 0 restraints, final R_1 = 0.0300 (based on F^2) for data with $I > 2\sigma(I)$ and, R_1 = 0.0343 on 1604 reflections, goodness-of-fit on F^2 = 1.031, largest electron density peak = 1.29 e·Å^{-3}.

X-ray Analysis of Complex 5. Crystal data: $C_{23}H_{38}N_3P_2BrPt$, orange, 0.1 × 0.1 × 0.05 mm^3, the crystal is refined like a twin, monoclinic, Cc, a = 6.993(2) Å, b = 28.041(6) Å, c = 13.723(3) Å, β = 94.46(3)°, T = 120(2) K, V = 2682.8(9) Å^3, Z = 4, fw = 693.5, D_c = 1.717 Mg·m^{-3}, μ = 6.854 mm^{-1}.

Data collection and processing: Nonius KappaCCD diffractometer, Mo Kα (λ = 0.71073 Å), graphite monochromator, $0 \le h \le 9$, $0 \le k \le 36$, $-17 \le l \le 17$, frame scan width = 2.0°, scan speed 1.0° per 30 s, typical peak mosaicity 0.88°, 25276 reflections collected, 3139 independent reflections (R_{int} = 0.083). The data were processed with Denzo-Scalepack.

Solution and refinement: The structure has been solved by the Patterson method with SHELXS-97.[13] Full matrix least-squares refinement based on F^2 with SHELXL-97, 273 parameters with 3 restraints, final R_1 = 0.0269 (based on F^2) for data with $I > 2\sigma(I)$ and, R_1 = 0.0298 on 3075 reflections, goodness-of-fit on F^2 = 1.049, largest electron density peak = 2.346.

Computational Methods. All DFT calculations were carried out using Gaussian 03, Revision C.02.[14] We used the PBE0 DFT exchange−correlation functional,[15] also known as PBE1PBE. PBE0 is the hybrid variant of PBE, Perdew, Burke, and Ernzerhof's nonempirical GGA functional, and contains 25% HF exchange. This functional yields more reliable reaction barrier heights than B3LYP[16] or other "conventional" exchange−correlation functionals,

(11) For NMR of complex **12** see: (a) Coulson, D. R. *J. Am. Chem. Soc.* **1976**, *98*, 3111. (b) Romeo, R.; Minniti, D.; Trozzi, M. *Inorg. Chem.* **1976**, *15*, 1134.

(12) For NMR data of complexes **12**−**14**, see: Arnold, D. P.; Bennett, M. A. *Inorg. Chem.* **1984**, *23*, 2117.

(13) Sheldrick, G. M. *SHELXL-97*, Program for Crystal Structure Determination; University of Göttingen: Göttingen, Germany, 1997.

(14) Frisch, M. J.; Trucks, G. W.; Schlegel, H. B.; Scuseria, G. E.; Robb, M. A.; Cheeseman, J. R.; Montgomery, J. A., Jr.; Vreven, T.; Kudin, K. N.; Burant, J. C.; Millam, J. M.; Iyengar, S. S.; Tomasi, J.; Barone, V.; Mennucci, B.; Cossi, M.; Scalmani, G.; Rega, N.; Petersson, G. A.; Nakatsuji, H.; Hada, M.; Ehara, M.; Toyota, K.; Fukuda, R.; Hasegawa, J.; Ishida, M.; Nakajima, T.; Honda, Y.; Kitao, O.; Nakai, H.; Klene, M.; Li, X.; Knox, J. E.; Hratchian, H. P.; Cross, J. B.; Bakken, V.; Adamo, C.; Jaramillo, J.; Gomperts, R.; Stratmann, R. E.; Yazyev, O.; Austin, A. J.; Cammi, R.; Pomelli, C.; Ochterski, J. W.; Ayala, P. Y.; Morokuma, K.; Voth, G. A.; Salvador, P.; Dannenberg, J. J.; Zakrzewski, V. G.; Dapprich, S.; Daniels, A. D.; Strain, M. C.; Farkas, O.; Malick, D. K.; Rabuck, A. D.; Raghavachari, K.; Foresman, J. B.; Ortiz, J. V.; Cui, Q.; Baboul, A. G.; Clifford, S.; Cioslowski, J.; Stefanov, B. B.; Liu, G.; Liashenko, A.; Piskorz, P.; Komaromi, I.; Martin, R. L.; Fox, D. J.; Keith, T.; Al-Laham, M. A.; Peng, C. Y.; Nanayakkara, A.; Challacombe, M.; Gill, P. M. W.; Johnson, B.; Chen, W.; Wong, M. W.; Gonzalez, C.; Pople, J. A. *Gaussian 03*, Revision C.02; Gaussian, Inc.: Wallingford, CT, 2004.

(15) Perdew, J. P.; Burke, K.; Ernzerhof, M. *Phys. Rev. Lett.* **1996**, *77*, 3865.

(16) Stevens, P. J.; Devlin, F. J.; Chabalowski, C. F.; Frisch, M. J. *J. Phys. Chem.* **1994**, *98*, 11623.

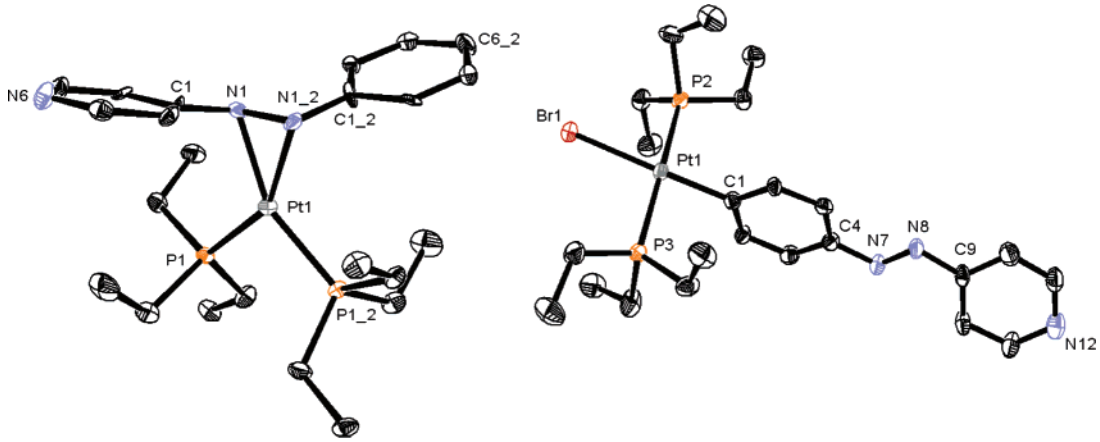

Figure 1. ORTEP diagram of **4** (left) and **5** (right) with thermal ellipsoids set at 50% probability. Hydrogen atoms are omitted for clarity. There is 1/2 molecule of **4** per asymmetric unit and atom C(1_2) etc. are generated by symmetry (symmetry transformations used to generate equivalents atoms #1 −x+1, −y+1, z; #2 −x+1, y−1/2, −z+1: #3 −x+1/2, y+1/2, −z+1). Selected bond lengths (Å) and angles (deg): For **4**: Pt(1)−N(1) 2.100(6), Pt(1)−N(1_2) 2.101(6), Pt(1)−P(1) 2.2516(19), Pt(1)−P(1_2) 2.2516(19), C(1)−N(1) 1.412(10), N(1)−N(1_2) 1.430(13), N(1_2)−Pt(1)−N(1) 39.8(3), N(1)−Pt(1)−P(1_2) 150.42 (18), N(1)−Pt(1)−P(1) 110.64(17), N(1_2)−Pt(1)−P(1) 150.42(18), P(1)−Pt(1)−P(1_2) 09.03(10). For **5**: Pt(1)−Br(1) 2.5302(11), Pt(1)−C(1) 2.009(8), C(4)−N(7) 1.418 (10), N(7)−N(8) 1.260(9), N(8)−C(9) 1.433(10), Pt(1)−P(2) 2.306(2), Pt(1)−P(3) 2.316(2); C(1)−Pt(1)−P(2) 91.6(2), C(1)−Pt(1)−P(3) 87.6(2), P(2)−Pt(1)−P(3) 172.28(9), C(1)−Pt(1)−Br(1) 178.7(2), P(2)−Pt(1)−Br(1) 87.13(6), P(3)−Pt(1)−Br(1) 93.67(6).[31]

Scheme 1. Selective Formation of Complexes 2, 4, and 7 by η^2-Coordination Followed by Oxidative Addition (for 2 and 7) to afford Complexes 5 and 8, respectively

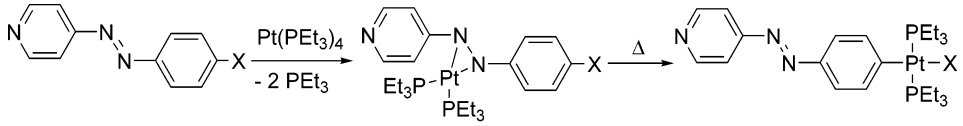

1, X = Br
3, X = H
6, X = I

2, X = Br
4, X = H
7, X= I

5, X= Br
8, X= I

without sacrificing performance of other properties.[17] With this functional, two basis set−RECP (relativistic effective core potential) combinations were used. The first, denoted SDD, is the combination of the Huzinaga−Dunning double-ζ basis set[18] on lighter elements with the Stuttgart−Dresden basis set−RECP combination[19] on transition metals. The second, denoted SDB-cc-pVDZ, combines the Dunning cc-pVDZ basis set[20] on the main group elements and the Stuttgart−Dresden basis set−RECP[19] on the transition metals with an added f-type polarization exponent taken as the geometric average of the two f-exponents given in the appendix of ref 21. Geometry optimizations were carried out using the former basis set, while the energetics of the reaction were calculated at these geometries with the latter basis set. Bulk solvent effects[22] were approximated by single-point PBE0/SDB-cc-pVDZ energy calculations using a polarized continuum (overlapping spheres) model (PCM)[23−25] with THF as the solvent, as in the experiments. The connectivity of the transition states was confirmed by performing intrinsic reaction coordinate (IRC) calculations.[26−28] Geometries were optimized using the default pruned (75 302) grid or when necessary for convergence with the "ultrafine" grid, i.e., a pruned (99 590) grid.

Results and Discussion

An equimolar amount of $Pt(PEt_3)_4$[29] and 4-(bromo-phenyl)-pyridin-4-yl-diazene (**1**)[10] were reacted in dry THF-d_8 at room temperature, resulting in the quantitative formation of complex **2** and 2 equiv of PEt_3 within 0.5 h, as judged by ^1H and $^{31}P\{^1H\}$ NMR spectroscopy (Scheme 1). Complex **2** and a recently isolated stilbazole complex exhibit nearly identical spectroscopic properties.[6,30] Furthermore, reaction of phenyl-pyridin-4-yl-diazene (**3**)[10] with $Pt(PEt_3)_4$ resulted in the formation of the isostructural complex **4**, which has been isolated and characterized by ^1H, $^{13}C\{^1H\}$, and $^{31}P\{^1H\}$, mass spectrometry, elemental analysis, and X-ray diffraction (Figure 1).[31] Complex **2** converts slowly into complex **5** at room temperature (e.g., 75% conversion after 96 h), which has been isolated and characterized by the same means as **4**.[31,32] Likewise, reaction of an equimolar amount of $Pt(PEt_3)_4$ and 4-(iodo-phenyl)-pyridin-4-yl-diazene (**6**)[10] in THF-d_8 results first in quantitative η^2-coordination of

(17) Quintal, M. M.; Karton, A.; Iron, M. A.; Boese, A. D.; Martin, J. M. L. *J. Phys. Chem. A* **2006**, *110*, 709.
(18) Dunning, T. H., Jr.; Hay, P. J. *Modern Theoretical Chemistry*; Plenum: New York, 1976; Vol. 3, p 1.
(19) Dolg, M. Effective Core Potentials. In *Modern Methods and Algorithms of Quantum Chemistry*; John von Neumann Institute for Computing: Jülich, 2000; Vol. 1, p 479.
(20) Dunning, T. H., Jr. *J. Chem. Phys.* **1989**, *90*, 1007.
(21) Martin, J. M. L.; Sundermann, A. *J. Chem. Phys.* **2001**, *114*, 3408.
(22) Cramer, C. J. *Essentials of Computational Chemistry: Theories and Models*; John Wiley & Sons: Chichester, UK, 2002; p 347.
(23) Miertus, S.; Scrocco, E.; Tomasi, J. *Chem. Phys.* **1981**, *55*, 117.
(24) Cossi, M.; Barone, V.; Cammi, R.; Tomasi, J. *Chem. Phys. Lett.* **1996**, *255*, 327.
(25) Miertus, S.; Tomasi, J. *Chem. Phys.* **1982**, *65*, 239.
(26) Fukui, K. *Acc. Chem. Res.* **1981**, *14*, 363.
(27) Gonzalez, C.; Schlegel, H. B. *J. Chem. Phys.* **1989**, *90*, 2154.
(28) Gonzalez, C.; Schlegel, H. B. *J. Phys. Chem.* **1990**, *94*, 5523.
(29) Schunn, R. A. *Inorg. Chem.* **1976**, *15*, 208.
(30) (a) Cowan, R. L.; Trogler, W. C. *J. Am. Chem. Soc.* **1989**, *111*, 4750. (b) Ittel, S. D.; Ibers, J. A. *J. Organomet. Chem.* **1973**, *57*, 389. (c) Dickson, R. S.; Ibers, J. A. *J. Am. Chem. Soc.* **1972**, *94*, 2988.
(31) CCDC-629320 and -629321 contain the supplementary crystallographic data for this paper. These data can be obtained free of charge via www.ccdc.cam.ac.uk/conts/retrieving.html (or from the Cambridge Crystallographic Data Centre, 12 Union Road, Cambridge CB21EZ, UK; fax: (+44) 1223-336-033; or e-mail: deposit@ccdc.cam.ac.uk).
(32) Burdeniuk, J.; Milstein, D. *J. Organomet. Chem.* **1993**, *451*, 213.

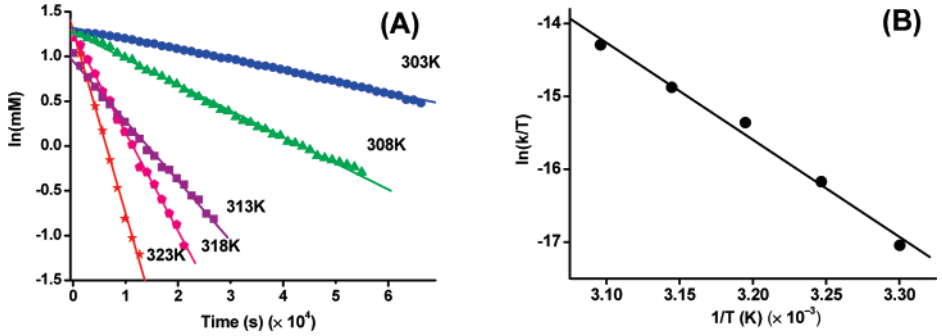

Figure 2. (A) $^{31}P\{^1H\}$ NMR follow-up measurements of the conversion of **2** → **5** in THF, 0.0289 M. (B) Eyring plot, $R^2 = 0.989$.

the metal center to the N═N moiety to afford complex **7** prior to activation of the Ar−I bond (**8**), as judged by low-temperature ^1H and $^{31}P\{^1H\}$ NMR spectroscopy (range: −65−0 °C). Evidently, η^2-coordination of $Pt(PEt_3)_2$ to the N═N moiety of **1** and **6** is kinetically preferable over the formation of complexes **2** and **7**, which involves the activation of the aryl−Br and aryl−I bonds (bond dissociation energy (BDE), Ph−Br = 80.5 kcal/mol, Ph−I = 65.5 kcal/mol).[33]

The thermolysis of complex **2** follows first-order kinetics in THF in the range 303−323 K with $\Delta G^{\ddagger}_{298K} = 24.6 \pm 1.6$ kcal/mol, $\Delta H^{\ddagger} = 26.5 \pm 1.6$ kcal/mol, and $\Delta S^{\ddagger} = 6.6 \pm 5.0$ eu (Figure 2). Mechanistically, the transformation of **2** → **5** could proceed via $Pt(PEt_3)_2$ dissociation followed by activation of the aryl−Br bond. Alternatively, the reaction may involve a metal ring-walking process. The low entropy value rules out metal−ligand dissociation as the slow step and could be consistent with either an intramolecular process or metal−ligand dissociation followed by aryl−halide oxidative addition as the rate-determining step.[34] In either case, oxidative addition appears to be the rate-determining step since the iodide derivative (**7**) of complex **2** undergoes selective aryl−I activation at lower temperatures (88% conversion after ∼17 h at 288 K in THF).[35] Complex **2** is stable under these reaction conditions.

Solid-state formation of complex **5** from **2** was observed by thermolysis of a powder of complex **2** for 11 days at 74 °C, resulting in quantitative conversion to complex **5**. This temperature is well below the melting point of the powder (∼120 °C). No other products were observed by ^1H or $^{31}P\{^1H\}$ NMR spectroscopy. Similarly, nickel−anthracene complexes undergo intramolecular dynamic processes in the solid state.[36] Therefore, we conclude that an intramolecular mechanism is most likely.

As expected for a first-order process (in complex **2**), no significant concentration effect on *k* has been observed (Table 1). These observations could support either a unimolecular process or a dissociative pathway via the reversible formation of $Pt(PEt_3)_2$ and ligand **1**, with aryl−halide oxidative addition being the rate-determining step. The reaction kinetics and NMR line shapes are affected neither by the presence of 0−10 equiv of PEt_3 nor by 1 equiv of compound **1** (Tables 1 and 2). Bimolecular and PEt_3 dissociation processes would likely be affected by the presence of free ligand.[37] A pathway involving bimetallic complexes is unlikely. No coordination of Pt was observed by $^{31}P\{^1H\}$ NMR spectroscopy upon addition of 1 equiv of $Pt(PEt_3)_4$ to complex **5** (313 K in THF, ∼12 h).

Table 1. Kinetic Studies of Conversion of Complex 2 to 5 at 313 K in THF

	2, M	PEt_3, equiv	$k \times 10^{-5}$, s^{-1}
1	0.0289		6.7
2	0.0722	2	6.3
3	0.0289	2	6.3
4	0.0289	10	6.2

Table 2. Kinetic Studies of Competition Reactions between 2 and PhBr (9) at 313 K in THF

	2, M	PEt_3, equiv	**9**, equiv	**1**, equiv	product ratio (**5**:**12**)	k, s^{-1} ($\times 10^{-5}$)
1	0.0145		1		5:1	7.1
2	0.0145	10	1		45:1	6.9
3	0.0025		1		>65:1	6.3
4	0.0145		1	1	>65:1	7.9
5	0.0145			1	>65:1	6.3

In order to estimate the relative reactivity of **1** toward oxidative addition by zerovalent platinum, 5 equiv of compound **1** was reacted in dry THF at 40 °C with 1 equiv of $Pt(PEt_3)_4$ in the presence of 5 equiv of PhBr (**9**), *p*-CF_3PhBr (**10**), and *p*-NO_2-PhBr (**11**), respectively. Under these reaction conditions, the following product distributions were observed by $^{31}P\{^1H\}$ NMR spectroscopy after consumption of the platinum complex precursor: **5**:**12** = 1:0, **5**:**13** = 2.5:1, and **5**:**14** = 1:3. It appears that the electron-withdrawing azo-pyridyl substituent activates the aryl−Br moiety toward oxidative addition even more strongly than the electron-withdrawing CF_3 group, which has a Hammett constant of $\sigma = 0.54$ (Scheme 2).[38]

In order to illustrate the control of the reaction outcome afforded by this bond activation process, competition experiments were performed by reacting stoichiometric amounts of complex **2** and PhBr (**9**) in dry THF at 40 °C. The $^{31}P\{^1H\}$ NMR spectroscopy showed the quantitative formation of complexes **5** (83%) and the above-mentioned complex **12** (17%). This is dissimilar to the outcome of the reaction of compounds **1** and PhBr (**9**) with $Pt(PEt_3)_4$ (Scheme 2). Complexes **5** and **12** were identified by addition of authentic samples to the product solution. Interestingly, the formation of complex **12** can be suppressed to ∼2% by the addition of 10 equiv of PEt_3 to the system and is not observable at all upon the addition of 1 equiv of compound **1**. Decreasing the concentration of the

(33) Lide, D. R. *CRC Handbook of Chemistry and Physics*, 83rd ed.; CRC Press: Boca Raton, FL, 2002.

(34) Collman, J. P.; Hegedus, L. S.; Norton, J. R.; Finke, R. G. *Principles and Applications of Organotransition Metal Chemistry*; University Science Books: Mill Valley, CA, 1987.

(35) The reaction of $Pt(PEt_3)_4$ with a structurally related halogenated vinylarene also proceeds via a rate-determining aryl−Br oxidative addition step to the platinum center.[6]

(36) (a) Cadenbach, T.; Gemel, C.; Schmid, R.; Fischer, R. A. *J. Am. Chem. Soc.* **2005**, *127*, 17068. (b) Boese, R.; Stanger, A.; Stellberg, P.; Shazar, A. *Angew. Chem., Int. Ed.* **1993**, *32*, 1475. (c) For a review, see: Coville, N. J.; Cheng, L. *J. Organomet. Chem.* **1998**, *571*, 149.

(37) (a) Mann, B. E.; Musco, A. *Dalton Trans.* **1980**, 776. (b) Northcutt, T. O.; Wick, D. D.; Vetter, A. J.; Jones, W. D. *J. Am. Chem. Soc.* **2001**, *123*, 7257.

(38) Both azo and pyridyl moieties are electron-withdrawing; see: Hansch, C.; Leo, A.; Taft, R. W. *Chem. Rev.* **1991**, *91*, 165.

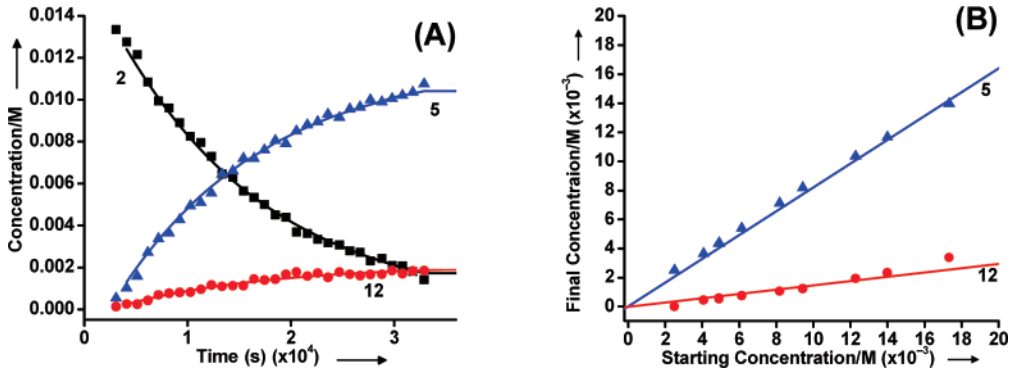

Figure 3. (A) Representative in situ $^{31}P\{^{1}H\}$ NMR follow-up measurements of the thermolysis of **2** (0.0145 M) in the presence of 1 equiv of PhBr (**9**) at 313 K in THF (experimental points) with fitted kinetic model as shown in Scheme 3 (solid lines). (B) Effect of varying initial concentration of reactants on concentration of **5** and **12** after 14 h (experimental points and model solid lines).

Scheme 2. Competitive Formation of Aryl−Pt(II) Complexes (5, 12−14)

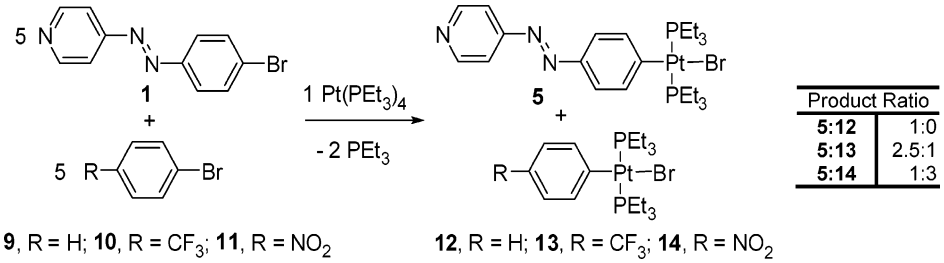

Product Ratio	
5:12	1:0
5:13	2.5:1
5:14	1:3

Scheme 3. Proposed Reaction Pathways for Competition Reaction between Compounds 2 and PhBr (9)[a]

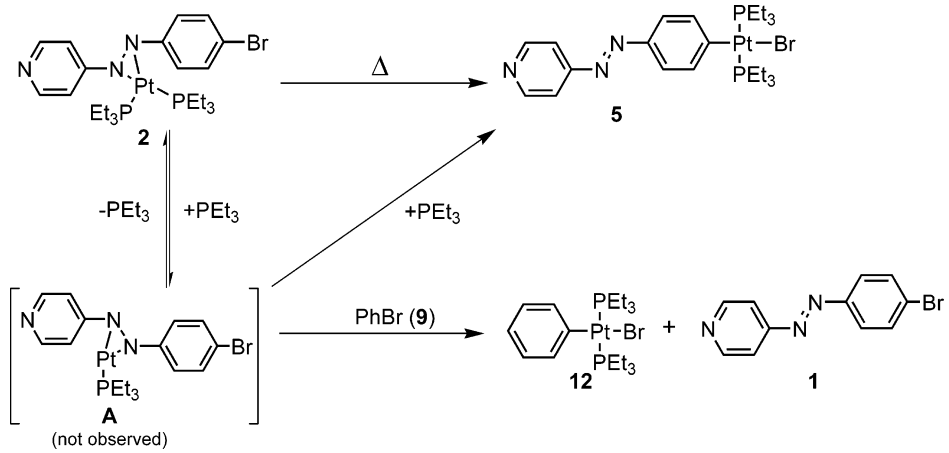

[a] The transformation **A** + PEt_3 → **5** might be a direct process and/or involve a reaction with ligand **1**.

starting materials also resulted in the exclusive formation of complex **5**. No intermediates were observed. Although complex **2** is the common precursor for both complexes **5** and **12**, our observations suggest that each is formed by a different and distinct pathway. For instance, a unimolecular mechanism for the formation of complex **5** and the bimolecular reaction of bromobenzene (**9**) with complex **2** for the formation of complex **12** may permit the a priori design of reaction systems to obtain desired products.

In order to elucidate the mechanism of the competition reaction between compounds **2** and **9**, the experimental data were fit to a number of multistep models numerically, using the Kintecus integrator.[39] Figure 3 shows (a) the fit of the model to the experimental kinetics data and (b) the predicted final concentration of **5** and **12** as a function of their starting concentration, compared with experimental values. Models were evaluated not only based on overall fit at the reaction conditions but also based on robustness of fit for a range of initial reactant concentration. The presented model was fit to kinetic follow-up $^{31}P\{^{1}H\}$ NMR measurements with a starting concentration of 0.0145 M (Figure 3A). This model was then run with various starting concentrations in the range 0.0025−0.25 M; the outputs are in excellent agreement with a series of experimental data (Figure 3B). Interestingly, this model includes the unimolecular ring-walking of complex **2** to **5**, as well as the rate-determining

(39) Ianni, J. C. *Kintecus*, Windows Version 2.80, 2002, can be found at http://www.kintecus.com. For examples of the use of Kintecus see: (a) Madhiri, N.; Olojo, R.; Simoyi, R. H. *Phys. Chem. Chem. Phys.* **2003**, *5*, 4149. (b) Greenvvald, E. E.; Park, J.; Anderson, K. C.; Kim, H.; Reich, B. J. E.; Miller, S. A.; Zhang, R.; North, S. W. *J. Phys. Chem. A* **2005**, *109*, 7915. (c) Zhang, L.; Callahan, K. M.; Derbyshire, D.; Dibble, T. S. *J. Phys. Chem. A* **2005**, *109*, 9232.

(40) (a) Dömling, A. *Chem. Rev.* **2006**, *106*, 17. (b) Ramón, D. J.; Yus, M. *Angew. Chem., Int. Ed.* **2005**, *44*, 1602. (c) Von Wangelin, A. J.; Neumann, H.; Gördes, D.; Klaus, S.; Strübing, D.; Beller, M. *Chem.−Eur. J.* **2003**, *9*, 4286.

(41) For a review, see: Keane, J. M.; Harman, W. D. *Organometallics* **2005**, *24*, 1786.

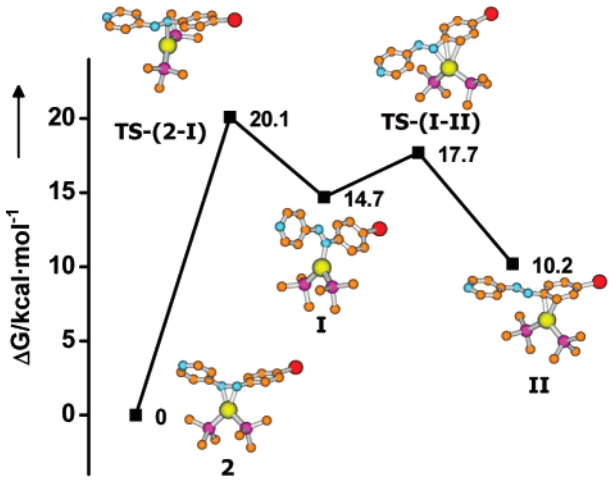

Figure 4. Free-energy pathways for ring-walking step as calculated at the PCM:PBE0/SDB-cc-pVDZ/PBE0/SDD level of theory utilizing the Gaussian03 program package. The ethyl substituents on the phosphine ligands have been replaced by methyl groups to reduce the computational cost. Hydrogen atoms are omitted for clarity. Atomic color scheme: Br, red; C, orange; N, light blue; Pt, yellow; P, pink.

dissociation of a phosphine of **2**, which eventually leads to the formation of **12**, via intermediate **A**, and provides an alternate minor route to **5** (Scheme 3). This is in good agreement with the experimental observation that performing the competition reaction in the presence of PEt_3 prevents the formation of complex **12**, whereas the intramolecular conversion of **2** to **5** is apparently unaffected. This model might not cover all mechanistic aspects of this reaction. However, *only models including an intramolecular conversion of **2** to **5** showed a possible fit.*

DFT calculations were performed to determine the transition states and the barriers connecting complex **2** and a metal−arene intermediate (Figure 4). Note that PMe_3 has been used instead of PEt_3 ligands. The movement of the metal center from the N═N unit to the arene involves a haptotropic rearrangement from η^2-N═N to η^1-N (**2** → **I**) via **TS-(2−I)** followed by η^2-coordination of the metal center to the arene (**II**). A similar haptotropic rearrangement for a structurally related stilbene system was not observed.[6] The transition-state geometry of the latter reveals metal η^3-coordination (**TS-(I−II)**). The ring-walking pathway is kinetically accessible via a coordination shift, as the energy barriers are sufficiently low. Transition states involving only one phosphine on the metal center have significantly higher energy barriers by 10−15 kcal/mol.

Summary and Conclusions

Platinum η^2-coordination to a N═N moiety is kinetically preferable over rate-determining oxidation addition of an aryl−halide bond. The process (**2** → **5**) is not affected by the concentration or presence of excess PEt_3 and proceeds also in the solid state. The relative reactivity of the azobenzene system (**1**) with a zerovalent platinum phosphine complex is PhBr (**9**) < *p*-CF_3PhBr (**10**) < **1** < *p*-NO_2PhBr (**11**). The facile coordination of the metal center to **1** can be exploited to direct the selectivity of aryl−halide bond activation processes. The presence of PEt_3 permits control of competitive aryl−bromide oxidative addition with PhBr (**9**) and complex **2**. Apparently, formation of products **5** and **12** proceed by dissimilar pathways. Series of competition experiments have been used to numerically derive a reaction model as shown in Scheme 3, which involves a unimolecular transformation of complex **2** to **5**. This ring-walking process is kinetically accessible, as shown by DFT calculations. We believe that the selectivity between the activation of aryl−halides in this model system demonstrates that the development of new synthetic strategies for selective chemical transformations via ring-walking processes may be possible.[9]

Acknowledgment. This research was supported by the Helen and Martin Kimmel Center for Molecular Design, Minerva, BMBF and MJRG. M.E.vd.B. is the incumbent of the Dewey David Stone and Harry Levine career development chair.

Supporting Information Available: Crystallographic data (CIF) for complexes **4** and **5**, kinetic model details, and full coordinates in *.xyz* format of all calculated complexes are available free of charge via the Internet at http://pubs.acs.org.

OM700519V